Hydration of the bromine ion in a supercritical 1:1 aqueous electrolyte

G. Ferlat, A. San Miguel, and J. F. Jal
Département de Physique des Matériaux, Université Claude Bernard-Lyon 1, F-69622 Villeurbanne, France

J. C. Soetens and Ph. A. Bopp
Laboratoire de Physico-Chimie Moléculaire, Université Bordeaux 1, (UMR 5803 CNRS), F-33405 Talence, France

I. Daniel and S. Guillot
Laboratoire de Sciences de la Terre, Université Claude Bernard, Lyon-1, 43 Boulevard du 11 novembre 1918, F-69622 Villeurbane, France

J. L. Hazemann and R. Argoud
Laboratoire de Cristallographie, Avenue des Martyres, BP166, F-38042 Grenoble, France
(Received 2 November 2000; published 6 March 2001)

Extended x-ray absorption fine structure (EXAFS) measurements have been carried out on 0.2 molal RbBr aqueous solutions at the Br-K edge from ambient to supercritical (SC) conditions, i.e., from density $\rho = 1.02$ to $\rho = 0.42$ g cm^{-3} and temperatures from 35 to 450 °C. Molecular dynamics (MD) simulations have been used to calculate EXAFS (MDXAS) spectra in ambient and SC conditions. The model used leads to an excellent agreement of the EXAFS spectra computed from the generated configurations with the experimental ones. Both show, in particular, a strong persistence of the Br^- ion first shell coordination at supercritical conditions. This result is in clear contrast with results found in the literature. The disagreement is interpreted as a consequence of a fundamental limitation of the use of the classic EXAFS perturbative techniques on such severely disordered fluids characterized by weak interatomic interactions and large local density concentration fluctuations.

DOI: 10.1103/PhysRevB.63.134202 PACS number(s): 61.10.Ht, 61.20.Ja, 61.20.Qg

I. INTRODUCTION

Supercritical fluids are currently the subject of an increasing interest in both fundamental and applied research.[1,2] Their unique properties allow their use as solvents, catalysts, and reactants, for instance for selective synthesis or toxic waste oxydation.[3] Among supercritical fluids, water and aqueous solutions play a crucial role in many biochemical or geological processes such as the release of fluids onto the seafloor or the formation of metal deposits.[4] These aspects, linked to solvation processes press for an accurate knowledge of hydrothermal solutions at a microscopic level. Until recently the only information available at a molecular level came from computer simulations, vibrational spectroscopies and NMR experiments . In the past few years, contributions from neutrons and x-ray related methods have emerged.[5,6]

However, there are still features which remain unclear both for supercritical water and aqueous solutions. Specifically, the large decrease of the water dielectric constant ϵ with decreasing density[7] is an indication of changes which take place in the hydrogen bond network and which may, as well, affect the ion solvation. The exact nature of these changes is still under discussion.[8] The difficulties arise from the multiplicity of the parameters involved (T,p and ρ) and their concomitant dependency, which can lead to opposite effects.[9] A decrease of ϵ should reinforce ion-ion interactions, giving rise to ion complexation.[10] However, in the near critical region of dilute solutions, it could be counterbalanced by strong aggregation of water molecules around the ion.[11] This is indeed the explanation considered usually for the observed density enhancement in attractive mixtures and for the large negative infinite dilution partial molar volume in the near critical region,[12] although another interpretation, based only on the pure solvent fluctuations, can be invoked.[13] In any case, both density fluctuations and solvent aggregation can lead to large local dielectric screening gradients[14] in the ion shell. One should consider these local distortions rather than the macroscopic quantity ϵ for an accurate description of the solvation characteristics.

The theoretical studies of supercritical 1:1 electrolyte solutions have been mostly restricted to NaCl solutions. However, they have been extended over a wide range of densities and temperatures from infinite dilution to moderate concentrations, using mainly molecular dynamics (MD) or Monte Carlo (MC) simulations.[9] In this paper, we shall focus on the description of the solvation structure of bromine ions in rather low concentrated supercritical solutions. One of the parameters needed for this description is the water coordination number for which, depending on the discussed properties, different definitions have been introduced.[9,15] For the purpose of comparison between simulations and experiments yielding the static structure, we shall mainly focus on the geometrically defined mean number of water molecules in the first hydration shell of an ion $n(r_{\text{ion-O}})$, called hereafter *coordination number*. It is thus defined by the following integral of the ion-water oxygen radial pair distribution function (RDF) $g_{XO}(r)$:

$$N_{XO} = n(r_{XO}) = 4\pi\rho_O \int_0^{r_{XO}} g_{XO}(r') r'^2 dr', \qquad (1)$$

where r_{XO} is the first minimum of $g_{XO}(r)$and ρ_O the number density of oxygen (water). The analog integral of the anion-water hydrogen RDF $g_{XH}(r)$first peak, N_{XH}, is thought to represent the amount of water molecules which are hydrogen bonded to the anion.

In the case of 1:1 electrolyte solutions, when approaching the critical region from the liquid state, the peaks in the ion-water RDF typically broaden and the minima become less well defined. This is in contrast with what is found for divalent ions, where the persistence of well-defined hydration shells can be observed.[16] The absence of deep minima between the RDF peaks in supercritical (SC) conditions introduces uncertainties in the definition of the ion shell radius r_{XO}, which will in turn influence the $n(r_{XO})$ values. This will be even more apparent on the anion-oxygen than on the cation-oxygen RDF as the inter atomic distances involved are larger in the anion case due to the orientation of the water molecules in the shell. When going from ambient to SC conditions, simulations show that the displacement of the first minimum in the anion-oxygen RDF is of the order of 1 Å towards larger values.[17,18] This increased width of the first hydration shell must be considered when comparisons of $n(r_{XO})$ are made between various states or various works, r_{XO} being either the same radius as in ambient conditions, r_{XO}^{amb}, or a larger one, r_{XO}^{SC}, corresponding to the apparent extension of the shell. However, simulations show that in spite of these general changes in the shape of the ion-water RDF with temperature and density, the ion coordination number remains essentially the same[16,18–20] when the integral in Eq. (1) is taken up to the actual minimum in $g_{XO}(r)$. Typically, for Cl^-, when going to SC conditions, the coordination number as defined by Eq. (1) remains almost constant or even increases and a reduction of about 20–30 % is found for $n_{ClH}(r)$.[16,20] A good discussion about the apparent paradox of simultanously increasing $n_{ClO}(r)$ and decreasing $n_{ClH}(r)$ can be found elsewhere.[21] Even at the high temperatures involved, the persistence of strong local properties like electric field or dielectric screening in the first ion shell due to strong local density enhancement has been postulated.[14] It has been found that extreme conditions (i.e., reduced density of 0.05 at the critical temperature) are necessary to remove half of the water molecules from the chloride ion first shell.[22] Although only few studies[16,17] have investigated the hydration of ions other than Cl^- and Na^+, these trends seem largely ion independent.

Unlike calculations, experimental data on the hydration of monovalent ions are still scarce due to difficulties to build up the high temperature and high pressure set up. Neutron diffraction isotopic substitution (NDIS) on aqueous solutions of $NiCl_2$ show a ~25% decrease of N_{ClD} from ambient conditions to $T=300\,°C$ and p=1000 bar.[23] It is worth to note that in the case of diffraction experiments, the definition of a coordination number obtained by $g(r)$ peak integration becomes even more arbitrary due to the fact that the partial RDF are generally overlapping in the total $G_{ion}(r)$. An illustration of these difficulties is given by the study of Cl^- hydration in LiCl solution[24,25] at $T=375\,°C$ and $p=1690$ bar. A Gaussian deconvolution applied to the first peak of $G_{Cl}(r)$ gave an unlikely number of 2.5 for N_{ClD} whereas an empirical potential structure refinement of the same data leads to a value of 3.8($\pm$0.3). This latter analysis gives a weak dehydration (~10%) as defined by N_{ClO}.

Previous studies of Rb^+ (Ref. 26) and Br^- (Ref. 27) hydration in RbBr solutions by extended x-ray absorption fine structure (EXAFS) spectroscopy yielded a more pronounced dehydration around these ions in SC conditions than what has been discussed so far. The number of neighbors was found to decrease from 5.6 at ambient conditions to 3.4 ($\pm$1.0) at $T=424\,°C$ and $p=383$ bar for Rb^+ in a 0.5 molal solution and from around 7 in ambient conditions to about 2–3 at $T=425\,°C$ and $p=412-500$ bar for Br^- in a large concentration range (0.02–1.5 mol). The EXAFS technique is mostly sensitive to the oxygen atoms of the water molecules. Since no counter ions were detected the coordination numbers can be identified to $n_{XO}(r_{XO})$. The ~40 and ~60 % reduction of the water coordination number, for Rb^+ and Br^-, respectively, clearly exceeds the above mentioned values.

In order to clarify this apparent contradiction, we have performed EXAFS experiments and MD simulations on 0.2 molal RbBr solutions. Using similar methods as in Refs. 26,27, we generated calculated EXAFS spectra from MD snapshots and compared them to experimental ones. Both were in good agreement, removing the apparent contradiction discussed above, since this procedure takes explicitly into account the large local structural fluctuations in these systems. Fundamental limitations to the use of the EXAFS conventional analysis have been recently reviewed.[28] Here, they will be stressed for systems characterized by large density or concentration fluctuations.

Section II will present the experimental conditions and Sec. III will describe the MD simulations and the calculation of the spectra. In Sec. IV and V, discussion of the results and general considerations for the study of SC systems will be addressed.

II. EXPERIMENTAL

X-ray absorption spectra for 0.2 mol RbBr solution have been acquired at the Br-*K* edge on a third generation synchrotron source in ambient conditions and along the $p=450$ bar isobar for four conditions of temperature ranging from $T=35\,°C$ to $T=450\,°C$. Data were taken at the BM32 EXAFS beamline at the ESRF (European Synchrotron Radiation Facility, Grenoble, France) working in transmission mode. A specially conceived hydrothermal autoclave with an internally heated amorphous sapphire cell was used in order to generate the high pressure and high temperature conditions. The vessel consists of a pressurized main cylinder vessel with two beryllium windows as x-ray entrances. The internal sapphire cell is placed at the center of the vessel in between the x-ray windows defining an x-ray path of 10 mm. Helium gas was used as pressurizing medium and *K* thermocouples allowed to monitor the sample temperature with an accuracy of $\pm 2°$. A pressure gauge with an accuracy of ± 3 bar provided the pressure reading. This set-up is very close to the one described in other works.[29,30] The aqueous solutions 0.2 molal of RbBr were introduced *ex situ* into the x-ray cavity of the sapphire cell that was afterwards placed in

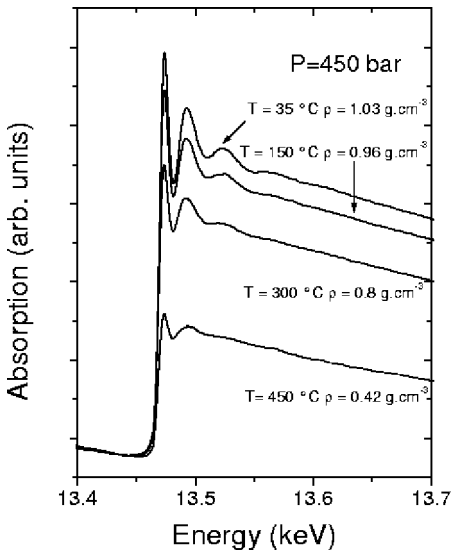

FIG. 1. EXAFS spectra along the $p=450$ bar isobar. From top to bottom, a series of temperature from $T=35\,^{\circ}\mathrm{C}$ to $T=450\,^{\circ}\mathrm{C}$.

the autoclave for the EXAFS experiment.

A double crystal Si (111) monochromator was used to scan the bending magnet x rays around the Bromine *K* edge (13474 eV). Sagittal focusing and a X-ray mirror were used to obtain a 0.2×0.2 mm^2 harmonic free spot on the sample. More details on the beamline characteristics can be found elsewhere.[31] Spectra were recorded following an optimized energy mesh scan at five different thermodynamic conditions: ambient conditions plus four different points at a 450 bar isobar (35,150,300,450 °C). These conditions are similar to some of the ones explored in Ref. 27. In order to improve the signal to noise ratio, three consecutive spectra were recorded for each thermodynamic point except at ambient conditions for which only one spectrum was recorded.

Figure 1 shows the spectra along the $p=450$ bar isobar. For clarity, the spectrum acquired in ambient conditions is not shown as it was perfectly superimposed with the (450 bar, 35 °C) one within the experimental accuracy. The density of the 0.2 m solution at ambient conditions can be obtained from Ref. 32 giving a value of $\rho=1.02$ g cm^{-3}. The evaluation of the experimental jump at the absorption edge allows to determine the fluid density for all others conditions and are reported in the same figure.

The Br-*K* edge is characterized by the presence of at least three well-defined multielectron excitations, noted *KN*, $KM_{4,5}$, and $KM_{2,3}$.[33–36] A proper account of these excitations is needed for a correct extraction of the EXAFS signal, especially in liquid matter where the structural signal is low.[37] The GNXAS package[38] was used for this purpose. A step-shaped function was used to empirically model the $KM_{4,5}$ edge with parameters that could be fixed to those determined for gaseous HBr within the error bars.[34,35] The *KN* edge was out of the low-*k* range used and the $KM_{2,3}$ was not discernible from the background, therefore they have not been included in our extraction of $\chi(k)$. Figure 2 shows the EXAFS $k\chi(k)$ spectra after extraction of the atomic background including the $KM_{4,5}$ multiple electron excitation. The

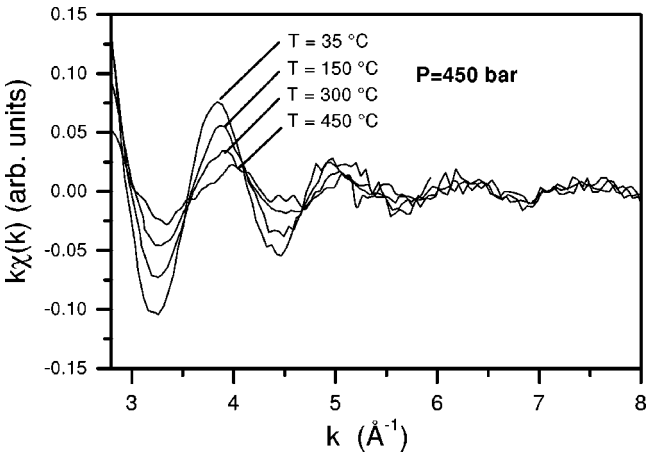

FIG. 2. *k*-weighted experimental EXAFS signals along the $p=450$ bar isobar. The $KM_{4,5}$ double electron excitation has been substracted (see text for details).

EXAFS signals obtained are comparable with the one given in Ref. 27.

III. METHODOLOGY

Molecular dynamics simulations have been performed for the same solution at ambient conditions $T=25\,^{\circ}\mathrm{C}$, $\rho=1.01$ g cm^{-3} and in the nearest critical conditions $T=450\,^{\circ}\mathrm{C}$, $\rho=0.40$ g cm^{-3}. Configurations from these simulations have been used to generate EXAFS spectra, which will be compared to the experimental spectra. The EXAFS data will not be subjected to any EXAFS analysis (fitting data within the classic EXAFS formula framework) for reasons discussed in Sec. IV.

A. Molecular dynamics simulation details

The potential functions used in the simulations are all pairwise additive. The SPC/*E* model of Berendsen *et al.*[39] is used to described water while the ions Rb^+ and Br^- are represented by a point charge and a Lennard-Jones (LJ) 12–6 center. The Rb^+-water potential parameters were derived by Åqvist from experimental hydration free energies using free energy perturbation simulations.[40] For Br^--water, we deduced a set of parameters from a study by Heinzinger.[41] Originally developed in conjunction with the ST2 water model, these parameters have been adapted in order to be used with the SPC/*E* water model. The list of parameters is given in Table I.

TABLE I. van der Waals parameters and partial charges used in the intermolecular potentials.

Atom	σ (Å)	ε (kJ mol^{-1})	$q(e)$
O	3.1656	0.65017	−0.8476
H			0.4238
Br^-	5.4661	0.07115	−1.0
Rb^+	5.6218	0.00071340	1.0

The SPC/*E* water model has been chosen because it represents a good compromise between computational efficiency (effective rigid three-sites model) and quality. In particular, the SPC/*E* model has been shown to give correct values of the static dielectric constant ϵ at room temperature[42,43] and along the liquid-vapor coexistence curve. Guissani *et al.*[44] found that the critical parameters for SPC/*E* are $T_c = 651.7$ K, $\rho_c = 0.326\ \mathrm{g\,cm^{-3}}$, and $p_c = 189$ bar, which are close to the experimental results ($T_c = 647.13$ K, $\rho_c = 0.322\ \mathrm{g\,cm^{-3}}$, and $p_c = 220.55$ bar).

The molecular dynamics simulations have been carried out at 25 and 450 °C with densities of $1.01\ \mathrm{g\,cm^{-3}}$ and $0.4\ \mathrm{g\,cm^{-3}}$, respectively, on systems consisting of two Rb^+Br^- ion pairs in a cubic box containing 452 water molecules (0.246 molal salt concentration) using periodic boundary conditions. During the simulation, a molecular cut off distance corresponding to half of the box length was applied for the non-Coulomb terms. The simulations were carried out using the MDPOL package[45] in the NEV ensemble. The trajectories were integrated using the velocity Verlet algorithm[46] and the bond lengths were kept rigid by employing the algorithm Rattle.[47] The long range electrostatic interactions were taken into account by the lattice summation method of Ladd[48–50] supplemented by the reaction field of a conductor ($\epsilon_{RF} = \infty$). The Ladd expansion is truncated after the term proportional to $(1/a)^{11}$, where a is the box edge. A time step of 2 fs was used and properties were collected during runs of 800 ps following an equilibration period.

B. MDXAS calculation details

EXAFS spectra can be generated from the real space output of MD simulations in two ways: (i) by calculating the spectrum from the averaged structure of the system, as described by the partial radial pair distribution functions[51] or (ii) by computing a series of EXAFS spectra from a series of instantaneous configurations of the system (snapshots) and averaging the spectra.[52]

The former method is faster and more straightforward. However, since in the supercritical state the instantaneous structures (at the time scale of the EXAFS experiment) can be dramatically different from the average one, the second method has been preferred here. In this latter case, snapshots are periodically saved during the MD simulation. Clusters of given radius, centered around the x-ray absorbing atoms (Br^-) are extracted and used to generate individual spectra. The average over all the individual spectra can then be directly compared to the experimental one. Similar studies can be found in the literature.[27,52–55] Snapshots were saved every 200 fs providing a total of 4000 spectra for each anion in the simulation box. A value of 7 Å for the radius of the clusters has been found to be sufficient to take into account all the significant contributions to the calculated signal. In order to save computer time, the standard overlapped atom potentials code FEFF6 (Ref. 56) was used to generate the EXAFS spectra. However, we checked on a restricted set of 250 configurations that no significant change for the amplitude of the signals is obtained using the *ab initio* self-consistent real space multiple-scattering code FEFF8.[57] As in previous studies,[27,52,53] the hydrogens have been removed from the configurations as they have been found to distort the FEFF calculations. Because of long time fluctuations of large amplitude in the SC system, particularly long simulations and a careful sampling are required to obtain reliable spectra. Test showed that a minimum of 1000 spectra is needed to obtain a meaningful average, thus the choice of using 4000 configurations, yielding 8000 spectra. A detailed investigation of these statistical aspects will be the subject of future work.

TABLE II. Simulation results. $\langle T\rangle$: average temperature during the simulation; $\langle U_{tot}\rangle$: average total potential energy of the solution; $\langle U_{species}\rangle$ potential energies between each species and all other ones, averaged values for one particle.

ρ/g cm^{-3}	1.01	0.40
box edge/Å	24.056	32.757
sampling/ps	800	800
$\langle T\rangle$/K	297.6	723.0
$\langle U_{tot}\rangle$/kJ mol^{-1}	−22236.4	−10055.9
$\langle U_{H_2O}\rangle$/kJ mol^{-1}	−46.39	−19.75
$\langle U_{Br^-}\rangle$/kJ mol^{-1}	−345.20	−283.38
$\langle U_{Rb^+}\rangle$/kJ mol^{-1}	−288.88	−281.09

IV. DISCUSSION

A. MD results

Typical results obtained from the simulations are given in Table II. A selection of some of the water-water, ion-water, and ion-ion RDF and their respective running coordination number obtained from the simulations are shown in Figs. 3 and 4 for both ambient and supercritical conditions. Charac-

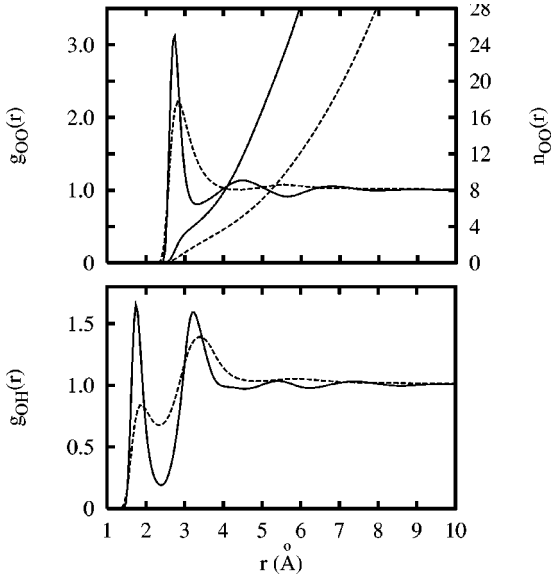

FIG. 3. Oxygen-oxygen and oxygen-hydrogen radial distribution functions of water. Solid line : ambient conditions (T=298 K, ρ=1.01 g cm^{-3}), dashed line: supercritical conditions (T=723 K, ρ=0.4 g cm^{-3}). The running coordination numbers are given for $g_{OO}(r)$ with the same convention.

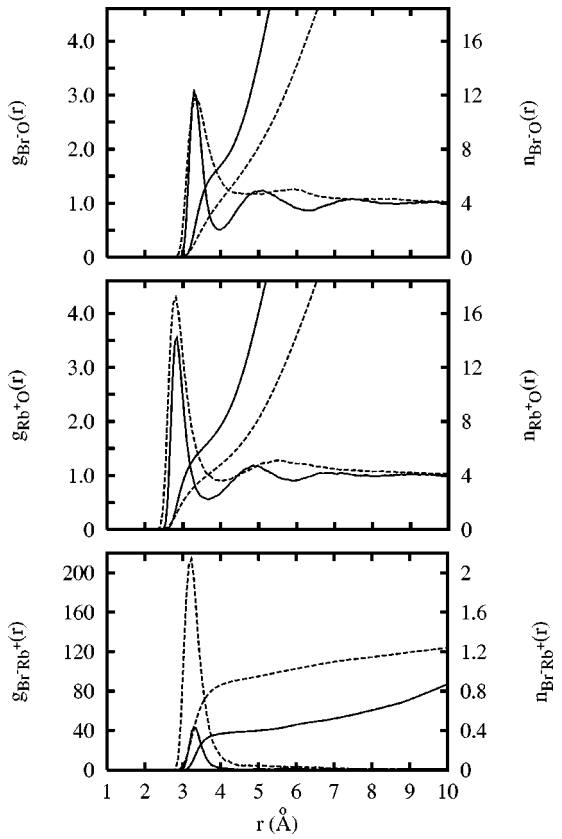

FIG. 4. Br-oxygen, Rb-oxygen, and Br-Rb radial distribution functions with running coordination numbers. Thermodynamics and lines convention are the same as in Fig. 3.

teristic data are listed in Table III. Values for the SC coordination number using the ambient RDF minimum are also provided for further discussion. Because of the low salt concentration, the water-water RDF of Fig. 3 are very close to those obtained for pure water in similar conditions.[58,59] Although considerably weakened, one can note the persistence, in SC conditions, of the $g_{OH}(r)$ first peak, related to the hydrogen bonds in the bulk water network.

The general trends of the Rb^+-water and Br^--water RDF are similar to those described in the Introduction. The Br-O RDF are in good agreement with the one obtained from a polarizable model[27] in almost similar thermodynamic conditions. In the latter case the noise does not allow to see the third shell in ambient conditions and the second shell in SC conditions due to the shorter time used in the simulations. In SC conditions, the ion-oxygen first peak maximum slightly shifts towards larger values in the anion case and towards lower values in the cation case, as it has been observed for NaCl solutions.[18] A significant broadening of the RDF first peak in SC conditions occurs for both ions. However the shift of the first peak minimum is weaker (0.4 Å) in the Rb^+-oxygen RDF than in the Br^--oxygen RDF (1 Å). Although partially filled, the first minimum remains observable in $g_{RbO}(r)$ whereas it has almost disappeared in $g_{BrO}(r)$. Compared to the $Na^+$and Cl^- cases,[16,18,20,60] this broadening effect is slightly enhanced due to the larger size of Rb^+ and Br^-.

The SPC/E model for water-water interaction is known to slightly overestimate the degree of structure in ambient conditions.[9,58] This trend could be enhanced in SC conditions as the constant dipole moment used in the model (2.35 D) starts to deviate from the real low density value. This should reflect on the ion-water interactions. However, the improvement using a polarizable model has been shown to be very small.[58] The enhanced thermal disorder in SC conditions leads to a weaker sensitivity to details of the potentials. The disagreement between experimental and model structures is likely to lie under the actual experimental accuracy of the EXAFS technique (see next subsection).

Using the RDF first minimum to define the coordination number leads to a slight increase from ambient to SC conditions of the number of oxygen atoms coordinating Br^- ($\sim$10%) while the equivalent number for Rb^+ decreases ($\sim$20%).

The similarity of the behavior of $g_{BrO}(r)$ and $g_{OO}(r)$ can be attributed to the negative charges of Br^- and O ($q_O = -0.85$ e for SPC/E model) and to the size of Br^-, which attenuates its solvation power. However, while the expansion of the first shell of a water molecule ($\sim$30%) follows closely the system expansion, the Br^- first shell expansion remains shorter ($\sim$20%).

Because of the uncertainties in the localization of the SC minima, the slight increase observed for the O and Br^- coordination numbers can be considered insignificant. A 10% decrease of the Br^--O number was obtained using a polarizable model.[27] The differences for the Br^--oxygen coordination number between the model used here (6.7 at 25 °C and 7.7 at 450 °C) and the model used in Wallen *et al.* study (5 at 25 °C and 4.5 at 425 °C) are most probably to be attributed to the shorter radii ($r_{Amb}=3.64$ Å and $r_{SC}=3.94$ Å) used in this case than to differences of models. Integrating

TABLE III. Characteristic values of the $g_{XO}(r)$ (X=O,Br^-,Rb^+) radial distribution functions. r_{XO}^{amb} and r_{XO}^{sc} denote the positions of the first minima in the radial distribution functions in ambient conditions (amb) and supercritical conditions (sc), respectively. The coordination number $n(r_{XO})$ is defined according to the following equation: $n(r_{XO})=4\pi\rho_O\int_0^{r_{XO}} g_{XO}(r')r'^2dr'$; see text.

	Ambient conditions		Supercritical conditions		
X	r_{XO}^{amb}	$n(r_{XO}^{amb})$	r_{XO}^{sc}	$n(r_{XO}^{sc})$	$n(r_{XO}^{amb})$
O	3.32 ($\pm$ 0.04)	4.4 ($\pm$ 0.2)	4.4 ($\pm$ 0.2)	4.8 ($\pm$ 0.6)	2.0 ($\pm$ 0.1)
Br^-	3.96 ($\pm$ 0.04)	6.7 ($\pm$ 0.2)	4.9 ($\pm$ 0.2)	7.7 ($\pm$ 1.0)	4.1 ($\pm$ 0.1)
Rb^+	3.65 ($\pm$ 0.03)	6.4 ($\pm$ 0.1)	4.0 ($\pm$ 0.1)	4.9 ($\pm$ 0.2)	4.0 ($\pm$ 0.1)

our RDF [Eq. (1)] up to these radii, values of 5 and 4.1 are obtained for ambient and SC conditions, respectively.

The persistence of the anion-oxygen coordination number from ambient to SC conditions is consistent with results obtained for Cl^- (Refs. 16,18,25) and OH^- (Ref. 16) in similar thermodynamic conditions. For Rb^+ in infinitely dilute conditions,[16] no change was observed, but the radii used were different.

On the other hand, using r_{XO}^{amb} to define the SC coordination number leads without ambiguity to a reduction which affects both ions by the same amount ($\sim 40\%$). Nonetheless this reduction is still smaller than the one experienced by water oxygen ($\sim 50\%$).

These values are close to those obtained using the $g_{XH}(r)$ first peak. Thus, the value for the coordination number using r_{XO}^{amb} carries a different type of information, linked to the proportion of water molecules strongly bonded to the ion, i.e., hydrogen bonded in the case of anions. This is consistent with a previous study of the Cl^- hydration structure[25] in which the broad SC Cl^--water first shell was found to be composed of about 5 water molecules with their O-H bond pointing towards the ion and about 4 ones apparently randomly oriented.

All ion-ion RDF are strongly enhanced in SC conditions, indicating the occurrence of much more stable ion complexes. The most significant change appears for $n_{BrRb}(r)$ which is close to 1 in SC conditions at a distance of the order of the expected Rb-Br first shell minimum (4.1 Å , from the ionic radii). This value is in good agreement with estimations from both MC simulations[10] and electrical conductance measurements[61] for NaCl solutions.

The broadening of the SC $g(r)$ functions is confirmed by visual inspection of the fluctuations of the ion environments as a function of the time. Figure 5 (lower part) shows the distribution of the Br^--O interatomic distances in the first coordination shell defined by the first minimum in $g(r)$. The upper part shows the Br^--O coordination number distribution inside the so-defined shell. The characteristic values (average, minimum, maximum and variance) for these distributions are summarized in Table IV. While the average coordination number are about 8 and 7 in ambient and SC conditions, respectively, extreme values of 2 and 15 are found sometimes in the SC case. We note that even in ambient conditions, the Br^- environment is far from being rigid. The adoption of an appropriate time scale to define a *dynamic hydration number*[15] in addition to the solely static defined coordination number should be of particular interest.

B. MDXAS results

Comparisons between the averaged calculated EXAFS spectra and the experimental ones in ambient and SC conditions are given in Fig. 6. The only fitting parameter has been the energy edge position E_0. The calculated edge position has been shifted by 2.9 ± 0.5 eV in the ambient calculation and 1.7 ± 0.3 eV in the supercritical one, both within the accuracy of the FEFF6 phase calculation. Our value for the SC Br^-–water coordination number (Table III) are significantly larger than the value previously published in an EXAFS analysis of similar spectra.[27] In almost the same conditions ($T = 425\,^\circ$C, $\rho = 0.42$ g cm^{-3}, and $p = 413$ bar), a value of $2.8(\pm 0.3)$ was obtained for the same solution (to be compared with our value ~ 8). Although short range sensitive, the EXAFS spectroscopy has been shown to give accurate values up to distances comparable to the photoelectron mean free path, i.e., about 5–7 Å. The coordination number ob-

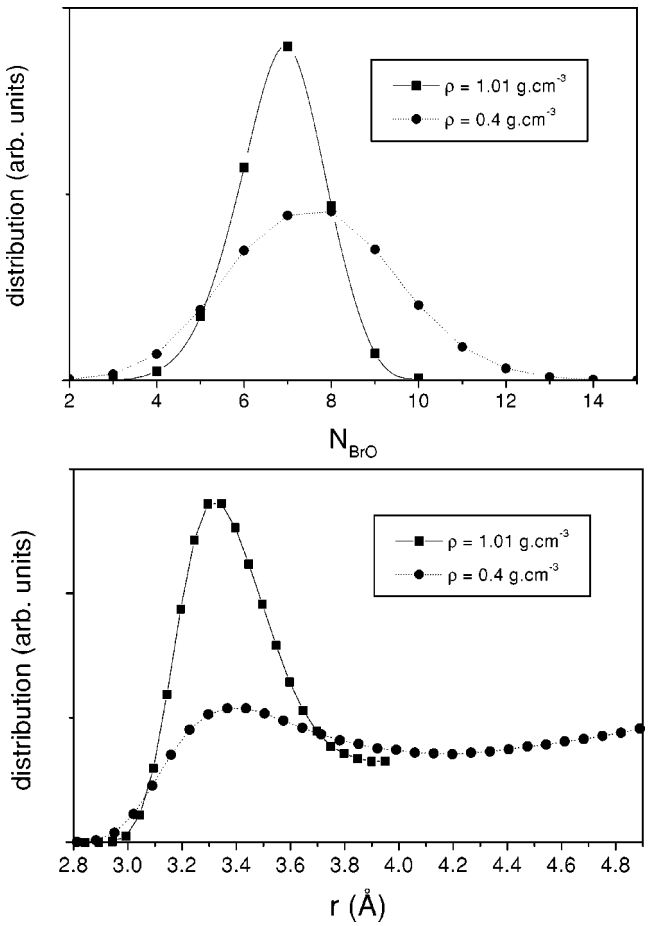

FIG. 5. Distribution of the number of water oxygens in the Br^- first coordination shell (see text) (top) and distribution of Br^--O interatomic distances (bottom) inside the so-defined shell, in ambient and supercritical conditions.

TABLE IV. Characteristic values (average, minimum, maximum, and variance) of the Br-O coordination numbers (N_{BrO}) and distance (R_{BrO}) distributions inside the Br^- first shell in ambient and supercritical conditions, see text.

	Ambient conditions	Supercritical conditions
$\langle N \rangle$	6.9	7.7
N^{min}	3	2
N^{max}	11	15
σ_N	1.0	1.9
$\langle R \rangle$	3.4	3.9
R^{min}	2.9	2.7
R^{max}	3.96	4.9
σ_R	0.2	0.6

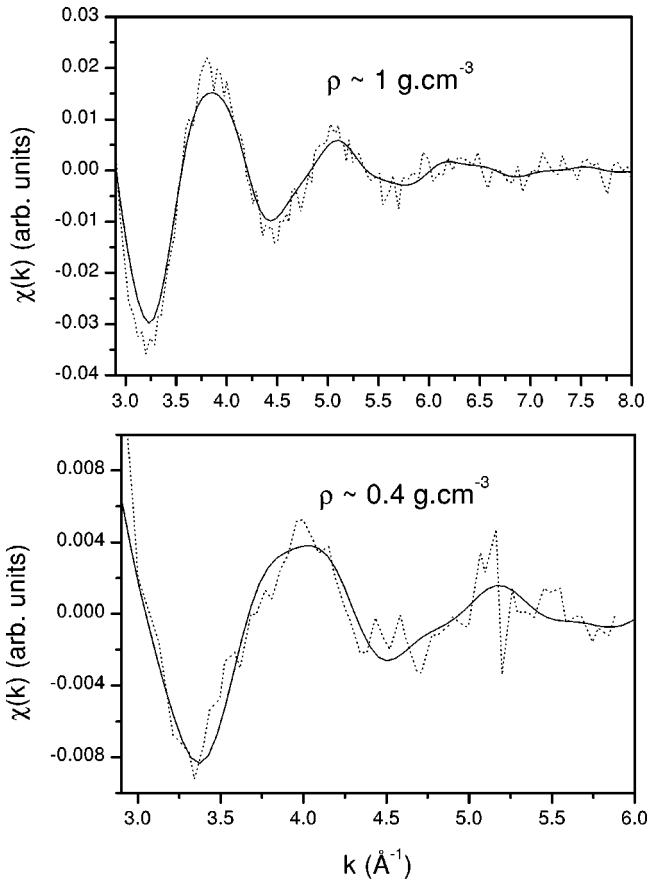

FIG. 6. Comparison of EXAFS experimental and calculated spectra. Top: at ambient conditions, bottom: at supercritical conditions (T = 450 °C). Calculated spectra are averages over 8000 individual spectra.

tained from EXAFS analysis should thus be comparable to $n_{\mathrm{BrO}}(r^{\mathrm{SC}})$, where r^{SC} is the first minimum of the SC ion-oxygen RDF.

The origin of this discrepancy can be understood when looking at the spectra calculated from instantaneous snapshots. As a result of the fluctuations of the local environment, the EXAFS signals calculated from individual snapshots differ drastically from each other. In Fig. 7 two of these signals are shown. They correspond to configurations, separated by 0.6 ps, and in which the Br^- shell (4.9 Å) was composed of 8 and 10 water molecules plus one Rb^+ ion. It can be seen that these signals are nearly out of phase. It has to be stressed that these 2 signals are given as an illustration and are by no means particular.

As a consequence of the spread of the various signal oscillations, the average spectrum results in a weaker signal amplitude than most of the individual spectra. A traditional EXAFS analysis of such a spectrum will therefore tend to provide a low coordination number as it is mainly connected to the amplitude of the signal in the standard EXAFS formula.

It may be worth reminding the reader that in the classic EXAFS formula, or its cummulant expansion, the effects of the disorder are treated in a perturbative way. The underlying assumption of a well-defined and only slightly perturbed

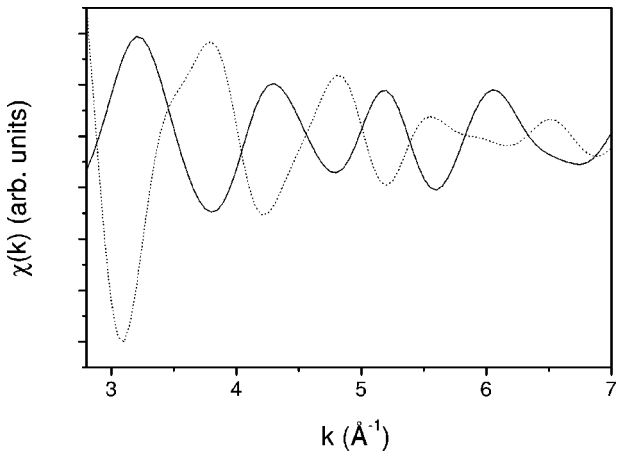

FIG. 7. Example of EXAFS calculated spectra obtained from 2 MD snapshots in supercritical conditions.

structure on any time scale greater than the photoelectron diffusion process is clearly not valid in supercritical aqueous monocharged electrolytes.

The inability of standard EXAFS analysis to provide reliable coordination numbers in such cases can also be understood from the results of Fig. 5. The variance of the Br^--O coordination number and interatomic distances distributions inside the Br^- first coordination shell are two to three times larger in SC conditions than in ambient ones. Moreover, the shape of the interatomic distances distributions is almost flat in SC conditions for distances between 3.8 and 4.9 Å. This means that the oxygens inside this region will give an incoherent contribution to the EXAFS signal. This corresponds to about half of the total oxygen atoms which are inside the Br^- first coordination shell. In others words, while the first coordination shell expands when going from ambient to SC conditions, giving almost the same coordination number, the effective contribution to the EXAFS signal in SC conditions arises from a more limited region and therefore will provide a lower value for the coordination number.

The work of Wallen *et al.*[27] was among the first to use MD snapshots to generate EXAFS spectra. The simulations were carried out using a polarizable model with ion parameters different from the one used here, and ran for 50 ps. The contradiction between dehydration derived from the $g(r)$ (10%) and from the EXAFS analysis (61%) was pointed out and attributed to the inaccuracy of the intermolecular potentials used in the simulations. It is shown here that the potentials are accurate enough to reproduce the experimental data within the experimental accuracy.

Comparisons between experimental and calculated EXAFS spectra in ambient conditions show a better agreement in our case than in Ref. 27. No comparison of SC spectra was provided in Ref. 27. In addition, the EXAFS calculated spectra were subjected to a classic perturbative EXAFS analysis and the value obtained in SC conditions (2.7) clearly disagrees with the result derived from $g_{\mathrm{BrO}}(r)$ (4.5). This was attributed to the limited number of configurations used. From our simulations, we observed indeed that this time is not sufficient to attain convergence. However, we add the more fundamental reason that a classic EXAFS analysis is

likely to give inaccurate results for both experimental and calculated spectra in such high-temperature conditions for the above evoked reason. It should be also noted from the results of Fig. 5 that even in ambient conditions the perturbative EXAFS analysis is not strictly valid. However, it has been shown to give very reliable results[62] as the deviation from the weak disorder framework has in this case only weak effects.

Thus, the currently used intermolecular potentials are able to provide realistic information on the solution structure in a wide range of conditions. However, because of the poor SC experimental signal to noise ratio, the comparison with simulated spectra is only possible on a limited and narrow k range and the precise evaluation of the error bars remains a difficult task. From the results of the Figs. 3 and 4, the less accurate and the less sensitive to the experimental comparison of Fig. 6 are the ion-ion results. Indeed, the contribution of Rb^+ and Br^- ions in the total EXAFS spectrum are weak in the k range studied. Removing the configurations in which contact-ion pairs or ion complexes occur from the calculation inputs does not result in a significant disagreement with experimental spectrum. Therefore although the proportion of contact ion pairs provided is in very good agreement with other experimental predictions, an experimental validation can not be provided here. Using the MDXAS technique on an extended set of solutions, an attempt to give confirmation of significant occurrence of ion-pairs in low concentrated 1:1 electrolytes in SC conditions will be the subject of another paper.[63]

V. CONCLUSIONS

New results for the hydration structure of the Br^- ion in a 0.2 molal RbBr supercritical solution have been derived combining EXAFS measurements and MD calculations. The experimental and simulated spectra are in excellent agreement, both at ambient and at SC conditions. A strong reduction of the EXAFS amplitude is observed with decreasing value of the sample density. This is in good agreement with previous experiments of Wallen *et al.*[27] They interpreted this as a reduction of the hydration number of Br^-. In contrast, our simulations show a persistence of a high amount of water molecules around the Br^- ion in the SC state, as it was experimentally observed in Cl^-.[23,25] The discrepancy between our results and those derived from classic EXAFS analysis[27] have been elucidated: the strong reduction of the EXAFS amplitude in SC conditions mainly arises from strong local structural fluctuations and not from a low number of neighbors around the ion. Simulations also show the formation of a significant amount of ion-pairs in SC conditions, but the reduced experimental sensitivity has not allowed a validation of this point. The peculiarity of the SC state is more likely to lie in instantaneous features than in averaged one. Thus, a full understanding of the SC structure of fluids should include consideration of instantaneous and dynamics properties. In addition to the classic correlation length and density fluctuation values, the characterization of the disorder has to be captured, for instance in terms of bond angles distribution, residence times as well as local densities fluctuations.

ACKNOWLEDGMENTS

We are grateful to Dr. S. de Panfilis for his help with the use of the GNXAS code. Financial support of the CNRS GDR Contract No. 1880 is also acknowledged. We thank J. Dupuy for interesting discussions.

[1] *Supercritical Fluids: Fundamentals and Applications*, Vol. 366 of *NATO Advanced Study Institute, Series E: Applied Sciences*, edited by E. Kiran, P. G. Debenedetti, and C. J. Peters (Kluwer Academic Publishers, Dordrecht, 2000).

[2] C. A. Eckert, B. L. Knutson, and P. G. Debenedetti, Nature (London) **383**, 313 (1996).

[3] L. T. Taylor, *Supercritical Fluid Extraction* (Wiley, New York, 1996), and references therein.

[4] J. V. Walther and J. Schott, Nature (London) **332**, 635 (1988).

[5] G. W. Neilson and J. E. Enderby, J. Phys. Chem. **100**, 1317 (1996).

[6] M. Nakahara, T. Yamaguchi, and H. Ohtaki, Recent Res. Devel. Phys. Chem. **1**, 17 (1997), and references therein.

[7] K. Tödheide, Ber. Bunsenges. Phys. Chem. **70**, 1022 (1966).

[8] C. H. Uffindell, A. Kolesnikov, J.-C. Li, and J. Mayers, Phys. Rev. B **62**, 5492 (2000).

[9] A. A. Chialvo and P. T. Cummings, in *Advances in Chemistry and Physics*, edited by I. Prigogine and S. A. Rice (Wiley, New York, 1999), Vol. 109, p. 115, and references therein.

[10] E. H. Oelkers and H. C. Helgeson, Science **261**, 888 (1993).

[11] O. Kajimoto, Chem. Rev. **99**, 355 (1999).

[12] C. A. Eckert, D. H. Ziger, K. P. Johnston, and S. Kim, J. Phys. Chem. **90**, 2738 (1986).

[13] E. Ruckenstein and I. Shulgin, J. Phys. Chem. B **104**, 2540 (2000).

[14] A. A. Chialvo, P. T. Cummings, J. M. Simonson, and R. E. Mesmer, J. Chem. Phys. **110**, 1064 (1999).

[15] R. W. Impey, P. A. Madden, and I. R. McDonald, J. Phys. Chem. **87**, 5071 (1983).

[16] P. B. Balbuena, K. P. Johnston, and P. J. Rossky, J. Phys. Chem. **100**, 2706 (1996).

[17] L. W. Flanagin, P. B. Balbuena, K. P. Johnston, and P. J. Rossky, J. Phys. Chem. B **101**, 2706 (1997).

[18] T. Driesner, T. M. Seward, and I. G. Tironi, Geochim. Cosmochim. Acta **62**, 3095 (1998).

[19] P. T. Cummings, H. D. Cochran, J. M. Simonson, R. E. Mesmer, and S. Karaborni, J. Chem. Phys. **94**, 5606 (1991).

[20] J. Gao, J. Phys. Chem. **98**, 6049 (1994).

[21] T. Driesner and P. T. Cummings, J. Chem. Phys. **111**, 5141 (1999).

[22] L. W. Flanagin, P. B. Balbuena, K. P. Johnston, and P. J. Rossky, J. Phys. Chem. **99**, 5196 (1995).

[23] P. H. K. de Jong, G. W. Neilson, and M. C. Bellisent-Funel, J. Phys. Chem. **105**, 5155 (1996).
[24] T. Yamaguchi, M. Yamagami, H. Ohzono, H. Wakita, and K. Yamanaka, Chem. Phys. Lett. **252**, 317 (1996).
[25] T. Yamaguchi and A. K. Soper, J. Chem. Phys. **110**, 3529 (1999).
[26] J. L. Fulton, D. M. Pfund, and S. L. Wallen, J. Chem. Phys. **105**, 2161 (1996).
[27] S. L. Wallen, B. J. Palmer, D. M. Pfund, J. L. Fulton, M. Newville, Y. Ma, and E. A. Stern, J. Phys. Chem. A **101**, 9632 (1997).
[28] A. Filipponi, J. Phys.: Condens. Matter **13**, R23 (2001).
[29] S. Hosokawa, K. Tamura, M. Inui, M. Yao, H. Endo, and H. Hoshino, J. Chem. Phys. **97**, 786 (1992).
[30] K. Tamura, M. Inui, and S. Hosokawa, Rev. Sci. Instrum. **95**, 1382 (1995).
[31] J. L. Hazemann, K. Nayouf, and F. de Bergevin, Nucl. Instrum. Methods Phys. Res. B **97**, 547 (1995).
[32] O. Sohnel and P. Novotny, *Densities of Aqueous Solutions of Inorganic Substances* (Elsevier, Amsterdam, 1985).
[33] G. Li, F. Bridges, and G. Brown, Phys. Rev. Lett. **68**, 1609 (1992).
[34] P. D'Angelo, A. Di Cicco, A. Filipponi, and N. Pavel, Phys. Rev. A **47**, 2055 (1993).
[35] P. D'Angelo, A. Di Nola, A. Filipponi, N. V. Pavel, and D. Roccatano, J. Chem. Phys. **100**, 985 (1994).
[36] Y. Ito, T. Mukoyama, S. Emura, M. Takahashi, S. Yoshikado, and K. Omote, Phys. Rev. A **51**, 303 (1995).
[37] A. Filipponi, Physica B **208&209**, 29 (1995).
[38] A. Filipponi, A. Di Cicco, T. Tyson, and C. R. Natoli, Solid State Commun. **78**, 265 (1991).
[39] H. J. C. Berendsen, J. R. Grigera, and T. P. Straatsma, J. Phys. Chem. **91**, 6269 (1987).
[40] J. Åqvist, J. Phys. Chem. **94**, 8021 (1990).
[41] K. Heinzinger, *Computer Modelling of Fluids Polymer and Solids* (Kluwer Academic Publishers, Dordrecht, 1990), pp. 357–394.
[42] M. R. Reddy and M. Berkowitz, Chem. Phys. Lett. **155**, 173 (1989).
[43] P. E. Smith and W. F. van Gunsteren, J. Chem. Phys. **100**, 3169 (1994).
[44] Y. Guissani and B. Guillot, J. Chem. Phys. **98**, 8221 (1993).
[45] J. C. Soetens, Ph.D. thesis, Université Henri Poincaré, Nancy I, 1996.
[46] W. C. Swop, H. C. Andersen, P. H. Berens, and K. R. Wilson, J. Chem. Phys. **76**, 637 (1982).
[47] H. C. Andersen, J. Comput. Phys. **52**, 24 (1983).
[48] A. J. C. Ladd, Mol. Phys. **33**, 1039 (1977).
[49] A. J. C. Ladd, Mol. Phys. **36**, 463 (1978).
[50] M. Neumann, Mol. Phys. **60**, 225 (1987).
[51] A. Filipponi, J. Phys.: Condens. Matter **6**, 8415 (1994).
[52] B. J. Palmer, D. M. Pfund, and J. L. Fulton, J. Phys. Chem. **100**, 13393 (1996).
[53] S. L. Wallen, B. J. Palmer, and J. L. Fulton, J. Chem. Phys. **108**, 4039 (1998).
[54] M. M. Hoffmann, J. G. Darab, B. J. Palmer, and J. L. Fulton, J. Phys. Chem. A **103**, 8471 (1999).
[55] J. Y. Raty, A. Saul, J. P. Gaspard, and C. Bichara, Phys. Rev. B **60**, 2441 (1999).
[56] J. Rehr and R. C. Albers, Phys. Rev. B **41**, 8139 (1990).
[57] A. L. Ankudinov, B. Ravel, J. J. Rehr, and S. D. Conradson, Phys. Rev. B **68**, 7565 (1998).
[58] P. Jedlovsky, J. P. Brodholt, F. Bruni, M. A. Ricci, A. K. Soper, and R. Vallauri, J. Chem. Phys. **108**, 8528 (1998).
[59] N. Matubayasi, C. Wakai, and M. Nakahara, J. Chem. Phys. **110**, 8000 (1999).
[60] P. T. Cummings, A. A. Chialvo, and H. D. Cochran, Chem. Eng. Sci. **49**, 2735 (1994).
[61] P. C. Ho, D. A. Palmer, and R. E. Mesmer, J. Solution Chem. **23**, 997 (1994).
[62] H. Ohtaki and R. Tamas, Chem. Rev. **93**, 1157 (1993).
[63] G. Ferlat, A. San Miguel, J.-F. Jal, J.-C. Soetens, P. A. Bopp, I. Daniel, S. Guillot, J.-L. Hazemann, and R. Argoud (unpublished).